

# Application of Experience-Based and MRI Radiomics in Differential Diagnosis of Benign and Malignant Pulmonary Nodules and Masses

Kaimin Tang, Yechun Zhang

Kunshan Rehabilitation Hospital, Kunshan 215300, Jiangsu, China

**Copyright:** © 2025 Author(s). This is an open-access article distributed under the terms of the Creative Commons Attribution License (CC BY 4.0), permitting distribution and reproduction in any medium, provided the original work is cited.

**Abstract:** *Objective:* To investigate the application of experience-based and Magnetic Resonance Imaging (MRI) radiomics in differentiating benign and malignant pulmonary nodules and masses. *Methods:* Sixty patients with pulmonary nodules or masses admitted from April 2024 to April 2025 were selected as study subjects. Surgical pathology was used as the gold standard to explore the differential diagnostic value of experience-based and MRI radiomics. *Results:* Twenty one MRI radiomic features were selected for screening, with 14 features removed and 7 remaining for normality testing. Using surgical pathology as the gold standard, among the 60 patients, 36 were benign and 24 were malignant, with detection rates of 60.00% and 40.00%, respectively. The detection rates of lobulation, vascular convergence sign, and GGO components in benign pulmonary nodules/masses were lower than those in malignant ones ( $P < 0.05$ ). The radiomics formula was  $\text{Radscore} = \text{Intercept} + \text{Weight (Feature)} \times \text{Feature}$ , with the calculated formula being  $\text{Radscore} = 0.16 - 0.32 \times \text{Sphericity} + 0.11 \times \text{Mass}$ . The AUC of the UTE Rad-score model was 0.672, which was lower than the AUC of the UTE nomogram (0.789) and the combined model (0.832) ( $P < 0.05$ ). *Conclusion:* Experience-based and MRI radiomics can play a significant role in differentiating benign and malignant pulmonary nodules and masses, with the combined model demonstrating more prominent diagnostic value.

**Keywords:** Pulmonary nodules; Magnetic resonance imaging; Radiomics

**Online publication:** August 4, 2025

## 1. Introduction

Lung cancer is one of the leading causes of cancer deaths globally<sup>[1]</sup>. Due to factors such as declining air quality and smoking, the incidence of lung cancer is increasing<sup>[2]</sup>. With the rapid development of clinical medicine, significant progress has been made in lung cancer treatment techniques, and survival rates have improved somewhat. To enhance the effectiveness of lung cancer treatment, it is crucial to improve diagnostic accuracy before treatment and select more appropriate and precise diagnostic methods to accurately identify lung cancer staging, type, degree of differentiation, etc. This provides rich information for clinical selection of more targeted treatment options<sup>[3]</sup>. Magnetic Resonance Imaging (MRI) is a highly regarded imaging technique with high tissue

resolution and no ionizing radiation. It can not only identify the presence of pulmonary nodule/mass lesions but also understand morphological changes <sup>[4]</sup>. With advancements in clinical medicine, MRI equipment has been upgraded, and various scanning techniques have been developed and clinically implemented. Thus, lung MRI examination has been widely used <sup>[5]</sup>. This study analyzed the application effect of experience-based and MRI radiomics in differentiating benign and malignant pulmonary nodules and masses.

## 2. Materials and methods

### 2.1. General information

Sixty patients with pulmonary nodules or masses admitted from April 2024 to April 2025 were selected as study subjects. There were 39 males and 21 females, aged 34-74 years, with an average age of  $(54.37 \pm 5.12)$  years. The lesion diameters ranged from 6.57 to 18.76 mm, with an average of  $(12.67 \pm 1.62)$  mm. Inclusion criteria: (1) Completed MRI imaging and surgical pathology examinations in our hospital; (2) Pulmonary nodule/mass diameter  $\geq 0.3$  cm; (3) Had complete clinical and pathological data; (4) Fully cooperated with clinical examinations. Exclusion criteria: (1) Low MRI image quality due to individual factors such as respiratory artifacts; (2) Presence of lung diseases that affect lesion evaluation, such as pulmonary tuberculosis, pneumonia, and pleural effusion; (3) Presence of other types of malignancies; (4) Did not meet the diagnostic criteria for pulmonary nodules/masses.

### 2.2. Methods

All subjects underwent MRI imaging examination, which are as follow:

- (1) Equipment and parameters: The equipment used was United Imaging MRI, model number uMR588.
- (2) Scanning sequence and scanning method: A 1.5T clinical magnetic resonance scanner and a 16-channel body phased array coil were selected for MRI imaging examination. Before the examination, respiratory training was conducted, and various imaging sequences were acquired, including coronal T2-weighted imaging (T2WI), axial T1-weighted imaging (presumably a typo, should be T1WI), diffusion-weighted imaging (DWI), respiratory-gated forward and reverse T1-weighted imaging, and isotropic T1-Quick-3D imaging. Sequential examination of lung nodules/lung masses was performed, and all image sequence data were collected and uploaded to a computer system. The image data was then retrieved for post-processing, and statistical analysis, comparison, application, and model creation for differential diagnosis of benign and malignant lung nodules/masses were completed using empirical methods and radiomics.

### 2.3. Observation indicators

- (1) Radiomic features of lung nodules/masses on MRI were screened and analyzed. The corrplot package in R language was used to draw a correlation coefficient diagram. Combined with Pearson's correlation coefficient, MRI imaging features with a correlation of  $|r| > 0.6$  were deleted, and the final radiomic features were obtained. Normality tests were performed, and the results were analyzed.
- (2) Based on the screening and analysis of radiomic features, two features were selected to create a radiomics model using the Lasso function. The Lasso function was used to convert the coefficients of unimportant radiomic features to 0. The function model was  $y_i = wTx_i + b$ , where  $y_i$  represents the prediction result,  $x_i$  corresponds to the values of each radiomic feature for  $y_i$ , and  $w$  is the coefficient of each radiomic feature.
- (3) The effectiveness and parameters of each radiomics model for predicting benign and malignant lung nodules/masses were evaluated. ROC curves were drawn, and various parameters were calculated.

## 2.4. Statistical methods

The data obtained in this study were expressed as mean  $\pm$  standard deviation and analyzed using SPSS 21.0 statistical software. Two-way analysis of variance (two-way ANOVA) was used for comparisons between the two groups, and one-way analysis of variance (one-way ANOVA) was used for comparisons within the group.  $P < 0.05$  was considered statistically significant. Radiomics and artificial intelligence deep learning are methods that use computer technology to deeply mine relevant imaging information within lesions and establish analytical models. Currently, there are many open-source software applications available. This project intends to use the Python-based Pyradiomics package for feature extraction, including first-order statistical features, shape features, second-order texture features, and features processed through filtering. After normalizing the original features, data preprocessing is performed using Z-score, mean normalization, and Pearson's correlation coefficient methods. Subsequently, support vector machines (SVM), multivariate logistic regression, and LASSO regression methods are applied to establish radiomics prediction models and combined models. Finally, the performance of the models is evaluated using the area under the receiver operating characteristic curve (AUC), accuracy, sensitivity, and specificity to obtain prediction models for benign and malignant lung nodules/masses. Separate prediction models and composite prediction models are developed for the differentiation of benign and malignant lung nodules/masses.

## 3. Results

### 3.1. Selection of MRI radiomics features for lung nodules/masses

Out of 21 MRI radiomics features selected for screening, 14 were eliminated, leaving 7 features for normality testing (Table 1). Using surgical pathology as the gold standard, among 60 patients, thirty-six were benign and 24 were malignant, with detection rates of 60.00% and 40.00%, respectively. The detection rates of lobulation, vascular convergence sign, and GGO components were lower in benign lung nodules/masses than in malignant ones ( $P < 0.05$ ). These three MRI radiomics features can be considered as the preferred options for differential diagnosis between benign and malignant lung nodules/masses (Table 2).

Based on the screening results of MRI radiomics features and the function formula, the radiomics formula obtained was  $\text{Radscore} = \text{Intercept} + \text{Weight}(\text{Feature}) \times \text{Feature}$ , where Intercept represents the Lasso function intercept, and Weight represents the coefficient of the radiomics feature collected by the Lasso function. The final calculation formula was  $\text{Radscore} = 0.16 - 0.32 \times \text{Sphericity} + 0.11 \times \text{Mass}$ .

**Table 1.** Selection of MRI radiomics features for lung nodules/masses

MRI radiomics feature	Kolmogorov-Smirnov	Shapiro-Wilk
Lobulation sign	0.004	0.000
Vascular convergence sign	0.010	0.000
Spiculation sign	0.200	0.622
Vacuole sign	1.792	1.777
Air bronchogram sign	0.050	0.100
GGO component	0.012	0.000
Pleural indentation sign	0.197	0.058

**Table 2.** Comparison of MRI radiomics features between benign and malignant lung nodules/masses

MRI radiomics feature	Benign (36 cases)	Malignant (24 cases)	$\chi^2$ value	<i>P</i> -value
Lobulation sign	16 (44.44)	19 (79.17)	7.143	0.008
Vascular convergence sign	5 (13.88)	11 (45.83)	7.514	0.006
Spiculation sign	10 (27.78)	7 (29.17)	0.014	0.907
Vacuole sign	12 (33.33)	8 (33.33)	0.000	1.000
Air bronchogram sign	14 (38.89)	9 (37.50)	0.012	0.914
GGO component	7 (19.44)	13 (54.17)	7.813	0.005
Pleural indentation sign	12 (33.33)	12 (50.00)	1.667	0.197

### 3.2. Efficacy and parameters of various radiomics models for predicting benign and malignant lung nodules/masses

The AUC of the UTE Rad-score model was 0.672, which was lower than the AUC of the UTE nomogram (0.789) and the combined model (0.832) ( $P < 0.05$ ). This indicates that the combined model has the best performance and the most prominent value in predicting benign and malignant lung nodules/masses (**Table 3**).

**Table 3.** Efficacy and parameters of various radiomics models for predicting benign and malignant lung nodules/masses

Radiomics model	AUC	SE	<i>P</i> -value	95% CI
UTE Rad-score model	0.672	0.062	0.041	0.500–0.743
UTE nomogram	0.789	0.045	0.002	0.693–0.885
Combined model	0.832	0.041	< 0.001	0.752–0.918

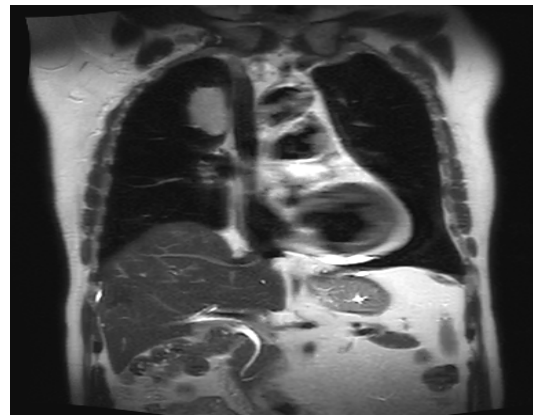
### 3.3. MRI images of malignant lung nodules

**Figure 1** represent a case of small cell lung cancer in the right upper lobe, with the diagnostic results indicating a mass in the anterior segment of the right upper lobe, significantly restricted diffusion with delayed enhancement of the lesion, suggesting a high possibility of right lung malignancy (MT). It is recommended to combine with bronchoscopy for further examination.

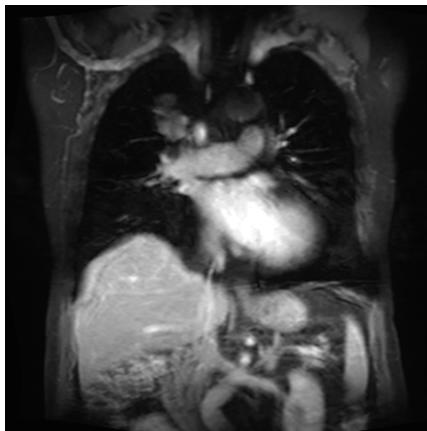




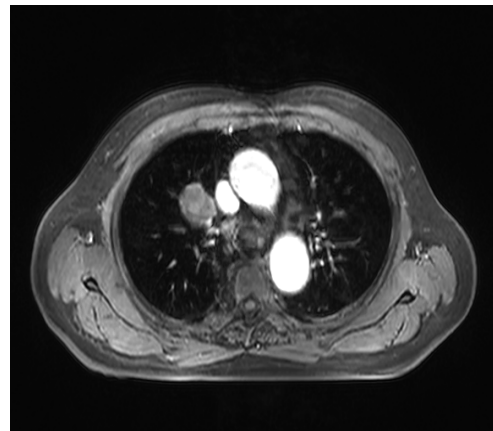
(a)



(b)



(c)



(d)

**Figure 1.** MRI imaging of small cell lung cancer in the right upper lobe; (a) T1; (b) T2 coronal view; (3) Coronal contrast-enhanced; (4) Enhanced axial plane

**Figure 2** represent a case of poorly differentiated adenocarcinoma in the left upper lobe, with the diagnostic results indicating a nodule in the left upper lobe, considering MT, possible MIA/IAC. It is recommended to combine with clinical symptoms and further diagnosis and treatment.

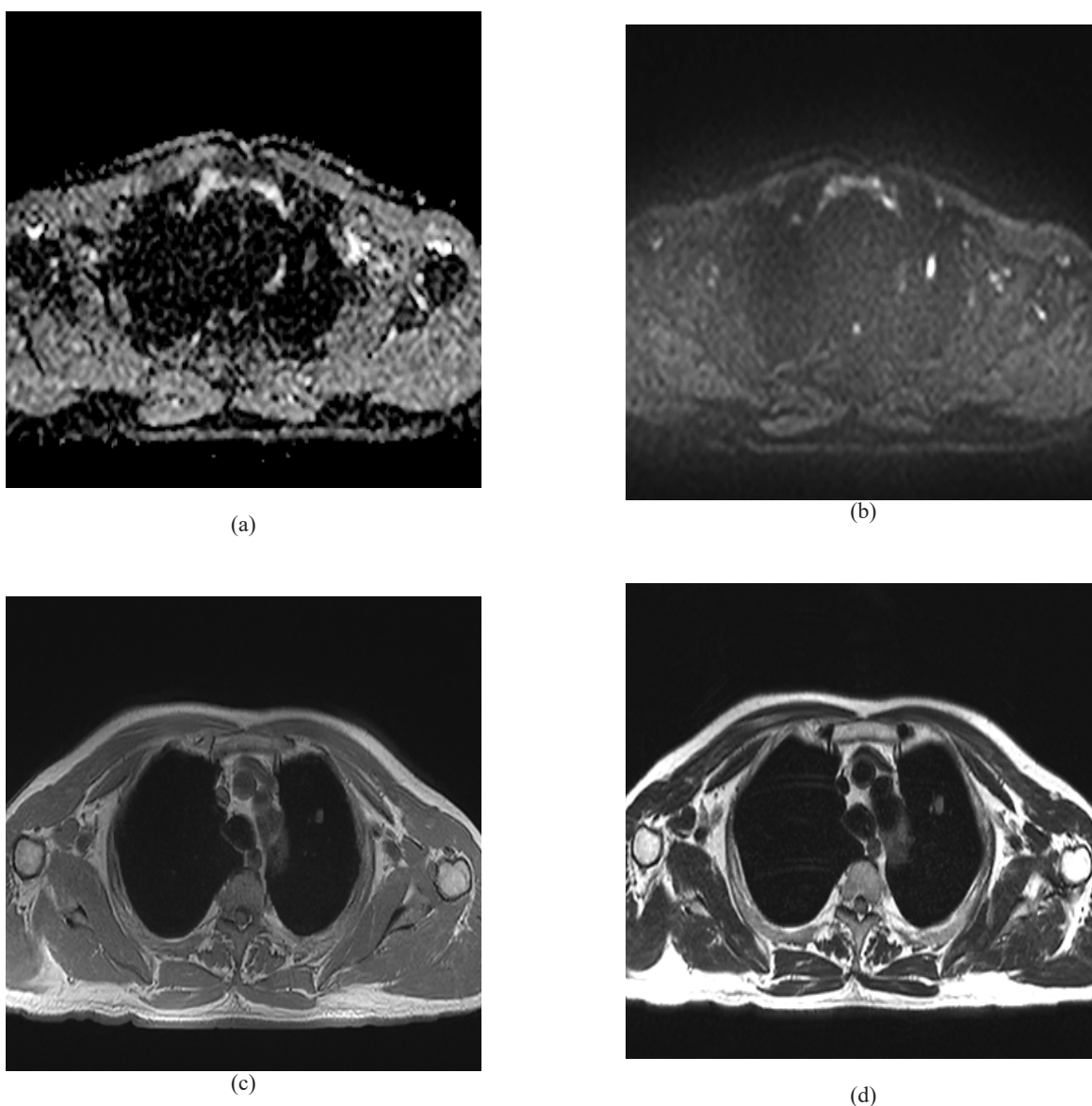


**Figure 2.** MRI imaging findings of poorly differentiated adenocarcinoma in the left upper lung; (a) ADC; (b) DWI; (c) T1; (d) T2

## 4. Discussion

“The 2019 National Cancer Report” shows that lung cancer has the highest incidence rate among malignant tumors in China <sup>[6]</sup>. Early-stage lung cancer does not present with obvious abnormal symptoms and often manifests as pulmonary nodules. Imaging scans can accurately identify pulmonary nodules/masses, but it is necessary to differentiate between benign and malignant lesions and select the most appropriate treatment plan based on the diagnostic results <sup>[7]</sup>. Some studies have pointed out that accurate preoperative evaluation of the nature of pulmonary nodules and identification of lung cancer lesions can improve the effectiveness of lung cancer treatment <sup>[8]</sup>. Nowadays, imaging technology has become an indispensable tool in the diagnosis and treatment of lung cancer, and MRI chest imaging has become an alternative and complementary means to conventional

radiological examination. Compared with CT diagnosis, MRI has advantages such as excellent soft tissue contrast, multi-parameter imaging, and safety without radiation. It can also comprehensively evaluate lung diseases through functional and structural imaging. The imaging mode functions and diagnostic information obtained can reflect the biophysical characteristics of tissues <sup>[9]</sup>.

MRI utilizes the resonance signal generated by atomic nuclei in a strong magnetic field to reconstruct images, providing high-contrast resolution of normal and abnormal tissues. It also has the characteristics of being sensitive to blood flow and having higher tissue resolution than spiral CT. This allows for accurate and clear presentation of some tissue features of tumor lesions, which is beneficial for qualitative examination of tumor lesions <sup>[10]</sup>. Currently, there are many scanning sequences for chest MRI with high sensitivity, so it is clinically believed that experience-based and MRI radiomics have high diagnostic value <sup>[11]</sup>. In this study, the detection rates of lobulation, vascular convergence sign, and GGO components in benign pulmonary nodules/masses were lower than those in malignant pulmonary nodules/masses ( $P < 0.05$ ), suggesting that MRI radiomics features can play a significant role in differentiating benign and malignant pulmonary nodules/masses, especially these three features <sup>[12]</sup>. The AUC of the UTE Rad-score model was 0.672, which was smaller than the AUC of the UTE nomogram (0.789) and the combined model (0.832) ( $P < 0.05$ ). This indicates that the combined model is more conducive to clinical differential diagnosis of diseases, with a larger AUC and more prominent efficiency.

## 5. Conclusion

In summary, experience-based and MRI radiomics can assist clinicians in accurately differentiating between benign and malignant pulmonary nodules and masses, guiding targeted clinical treatment of diseases.

## Disclosure statement

The authors declare no conflict of interest.

## References

- [1] Deng H, Zheng L, Wu D, et al., 2022, Observation of X-ray and MRI Diagnostic Imaging Features of Patients with Solitary Pulmonary Nodules. *Chinese Journal of CT and MRI*, 20(9): 58–59.
- [2] Jiang Y, Pu D, Yu N, 2023, Research Progress of Radiomics Based on Magnetic Resonance Imaging in Lung Cancer. *Journal of Magnetic Resonance Imaging*, 14(7): 166–170.
- [3] Yu B, Qian W, Li L, et al., 2025, Study on the Value of MRI Multi-b-Value DWI Quantitative Parameters in Diagnosing Benign and Malignant Solid Pulmonary Nodules. *Chinese Journal of CT and MRI*, 23(1): 63–65, 81.
- [4] Zhang J, Xiong Z, Li Z, 2023, Research Progress and Prospects of Ultra-Short Echo Time Magnetic Resonance Imaging for Pulmonary Nodules. *Journal of Magnetic Resonance Imaging*, 14(1): 183–188.
- [5] Wang X, Chen J, Gu H, et al., 2023, Study on the Differential Diagnosis Efficacy of Magnetic Resonance Diffusion-Weighted Imaging for Benign and Malignant Solitary Pulmonary Nodules. *China Medical Equipment*, 20(10): 80–84.
- [6] Xiang L, Qin Y, Yang H, et al., 2023, Value of IVIM-DWI Global Histogram Parameters in Differentiating Benign and Malignant Solitary Pulmonary Nodules. *Radiology Practice*, 38(12): 1539–1547.
- [7] Liu X, Kan X, Wang Y, et al., 2025, Application Value of MRI Multi-Parameter in Differential Diagnosis of Solid Solitary Pulmonary Nodules. *Journal of Clinical Radiology*, 44(1): 87–94.

- [8] Hu J, Liu M, Zhao W, et al., 2023, Diagnostic Value of T1WI Star-VIBE Enhancement Combined with TWIST-VIBE Dynamic Contrast-Enhanced MRI for Pulmonary Nodules. *Journal of Central South University (Medical Sciences)*, 48(4): 581–593.
- [9] Xia Z, Liu Z, Hu Q, et al., 2024, Construction and Validation of a Predictive Model for Lung Nodule Invasiveness Based on the XGBoost Machine Learning Algorithm: A Two-Center Study. *Chinese Journal of CT and MRI*, 22(8): 166–169.
- [10] Lou J, Meng S, Qin Q, et al., 2024, Exploring the Value of MRI and CT Haralick Texture Parameters in Diagnosing Benign and Malignant Pulmonary Nodules. *Chinese Journal of CT and MRI*, 22(7): 56–59.
- [11] Ma B, Zhu J, Chen J, et al., 2022, Discussion on the Clinical Value of MRI Examination in Differentiating the Nature of Solitary Pulmonary Nodule Lesions. *Chinese Journal of CT and MRI*, 20(8): 65–67.
- [12] Liu J, Jiang J, Yin J, et al., 2022, Differential Diagnosis of Benign and Malignant Pulmonary Nodules and Masses Based on Multimodal MR Radiomics. *Chinese Journal of Radiology*, 56(5): 542–548.

**Publisher's note**

Bio-Byword Scientific Publishing remains neutral with regard to jurisdictional claims in published maps and institutional affiliations.